Accepted Manuscript

Synthetic, enzyme kinetic, and protein crystallographic studies of *C*-β-D-glucopyranosyl pyrroles and imidazoles reveal and explain low nanomolar inhibition of human liver glycogen phosphorylase

Anastassia L. Kantsadi, Éva Bokor, Sándor Kun, George A. Stravodimos, Demetra S.M. Chatzileontiadou, Demetres D. Leonidas, Éva Juhász-Tóth, Andrea Szakács, Gyula Batta, Tibor Docsa, Pál Gergely, László Somsák

Please cite this article as: A.L. Kantsadi, E. Bokor, S. Kun, G.A. Stravodimos, D.S.M. Chatzileontiadou, D.D. Leonidas, E. Juhász-Tóth, A. Szakács, G. Batta, T. Docsa, P. Gergely, L. Somsák, Synthetic, enzyme kinetic, and protein crystallographic studies of *C*-β-D-glucopyranosyl pyrroles and imidazoles reveal and explain low nanomolar inhibition of human liver glycogen phosphorylase, *European Journal of Medicinal Chemistry* (2016), doi: 10.1016/j.ejmech.2016.06.049.

Synthetic, enzyme kinetic, and protein crystallographic studies of *C*-β-D-glucopyranosyl pyrroles and imidazoles reveal and explain low nanomolar inhibition of human liver glycogen phosphorylase

A. L. Kantsadi, É. Bokor, S. Kun, G. A. Stravodimos, D. S.M. Chatzileontiadou, D. D. Leonidas, É. Juhász-Tóth, A. Szakács, Gy. Batta, T. Docsa, P. Gergely, and L. Somsák
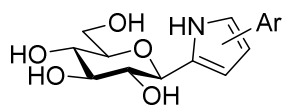
No inhibition

Best glucose derived inhibitors of human liver glycogen phosphorylase *a*

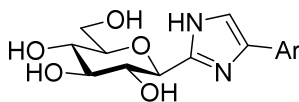| Ar	Ph	2-naphthyl
K_i [nM]	156	26

Synthetic, enzyme kinetic, and protein crystallographic studies of *C*-β-D-glucopyranosyl pyrroles and imidazoles reveal and explain low nanomolar inhibition of human liver glycogen phosphorylase

Anastassia L. Kantsadi,[1#] Éva Bokor,[2#] Sándor Kun,[2#] George A. Stravodimos,[1] Demetra S.M. Chatzileontiadou,[1] Demetres D. Leonidas,[1*] Éva Juhász-Tóth,[2] Andrea Szakács,[2] Gyula Batta,[2] Tibor Docsa,[3] Pál Gergely,[3] and László Somsák[2*]

[1]*Department of Biochemistry and Biotechnology, University of Thessaly, 26 Ploutonos Str. 41221 Larissa, Greece*

[2]*Department of Organic Chemistry, University of Debrecen, POB 400, H-4002 Debrecen, Hungary*

[3]*Department of Medical Chemistry, Faculty of Medicine, University of Debrecen, Egyetem tér 1, H-4032 Debrecen, Hungary*

[#]These authors have equally contributed to this work.

---

[*] Corresponding authors: DDL – tel. +302410565278, fax +302410565290, e-mail ddleonidas@bio.uth.gr;
LS – tel. +3652512900 ext 22348, fax +3652512744, e-mail somsak.laszlo@science.unideb.hu.

Abstract

C-β-D-Glucopyranosyl pyrrole derivatives were prepared in the reactions of pyrrole, 2-, and 3-aryl-pyrroles with *O*-peracetylated β-D-glucopyranosyl trichloroacetimidate, while 2-(β-D-glucopyranosyl) indole was obtained by a cross coupling of *O*-perbenzylated β-D-glucopyranosyl acetylene with *N*-tosyl-2-iodoaniline followed by spontaneous ring closure. An improved synthesis of *O*-perbenzoylated 2-(β-D-glucopyranosyl) imidazoles was achieved by reacting *C*-glucopyranosyl formimidates with α-aminoketones. The deprotected compounds were assayed with isoforms of glycogen phosphorylase (GP) to show no activity of the pyrroles against rabbit muscle GPb. The imidazoles proved to be the best known glucose derived inhibitors of not only the muscle enzymes (both a and b) but also of the pharmacologically relevant human liver GPa (K_i = 156 and 26 nM for the 4(5)-phenyl and -(2-naphthyl) derivatives, respectively). An X-ray crystallographic study of the rmGPb-imidazole complexes revealed structural features of the strong binding, and also allowed to explain the absence of inhibition for the pyrrole derivatives.
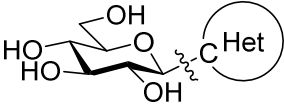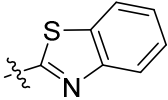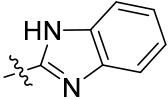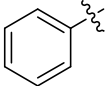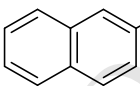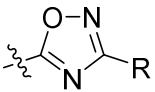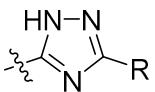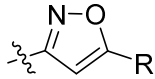
Keywords: Diabetes type 2; Glycogen phosphorylase inhibitor; *C*-Glucopyranosyl derivative; Pyrrole; Indole; Imidazole.
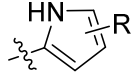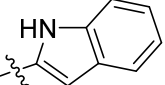
Introduction

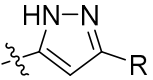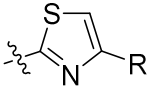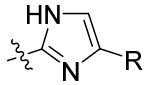A key player in glycogen metabolism is glycogen phosphorylase (GP; EC 2.4.1.1), an enzyme that catalyses glycogen degradation to glucose-1-phosphate (Glc-1-P).[1] Three isoforms of GP exist in the brain, muscle and liver tissue that share ~80 % sequence homology. GP is controlled by allosteric effectors and reversible phosphorylation. It exists in at least two inter-convertible forms, a low activity and substrate specificity T state and a high activity and substrate specificity R state, which are in equilibrium. Phosphorylation by glycogen phosphorylase kinase (PhK) or the binding of various allosteric activators, such as AMP, shift the equilibrium towards the R state. In contrast, dephosphorylation by glycogen phosphorylase phosphatase or the binding of inhibitors such as glucose promote the transition from the R to T state. The active phosphorylated enzyme (GPa) is the main form of GP in the liver whereas the unphosphorylated inactive form (GPb) is the prevalent form in the resting muscle. Extensive conformational changes occur in the tertiary structure upon transition from the T to R state.[2, 3] These mainly occur at the inter-subunit interface and result in the rearrangement of the flexible 280s loop (residues 282 to 285) from a conformation that blocks access to the catalytic site of the enzyme (T state) to one that allows substrate binding (R state). X-ray crystallographic studies have revealed that apart from the catalytic site there are other six different ligand binding sites: the allosteric site, the new allosteric site, the inhibitor site, the glycogen storage site, the benzimidazole site and the quercetin binding site.[4, 5] Although AMP binds to both the muscle and the liver enzyme, only the muscle isozyme is activated cooperatively.[6] There are no insertions or deletions in the sequence of the liver enzyme as compared to the muscle and out of the 171 amino acid differences between the two enzymes, 49% (85 amino-acids) are conservative and most of the amino acid changes are functionally neutral. The active site is conserved in both amino acid sequence and structural architecture.[6]

The liver is capable of storing glucose as glycogen and, through a reverse process, to produce and release glucose to the blood stream. Therefore, the liver is intimately linked to glycaemic control and human liver GP (hlGP) is a validated pharmaceutical target for the discovery of novel antihyperglycaemic agents.[1, 4, 7] Glycogen phosphorylase inhibitors (GPIs) have been shown to have a pharmaceutical potential to combat type 2 diabetes (the non-insulin dependent form of diabetes)[8-10] while they were also found to display cardioprotective effects[11, 12] and anticancer activity[13-16] as well as to reduce cerebral ischemia.[17, 18] The design of GPIs has mainly been focused on derivatives of glucose (the physiological inhibitor of the enzyme) and during the last decade, the active site of GP has been probed with more than 150 glucose derivatives.[1, 4, 19-24] The main goal of the design was to maximize the number of interactions with active site residues and thus increase inhibitory potency. In this context much effort has been devoted to introduce *C*-1 substituents suitable to exploit interactions with a hydrophobic cleft inside the active site, the so-called β-cavity. As a result of these studies, three compound classes emerged as submicromolar inhibitors of GP:[19, 23, 24] glucopyranosylidene-spiro-heterocycles, *N*-acyl-*N'*-β-D-glucopyranosyl ureas, and *C*-β-D-glucopyranosyl heterocycles. A collection of the latter type of compounds in Chart 1 allows one to conclude that the presence of a hydrogen-bond donor (HBD) heterocycle is in general a better inhibitor than the non-HBD counterpart (compare the pairs **1-2**,[25, 26] **3-4**,[27-30] **5-6**,[31] and **7-8**[31]). From these series *C*-β-D-glucopyranosyl imidazoles[31] **8** have so far shown the highest potency against rabbit muscle GPb (rmGPb). Similarly to the other two inhibitor classes, the *C*-β-D-glucopyranosyl compounds with a larger aromatic substituent (cf phenyl **a** *vs* naphthyl **b** derivatives in Chart 1) proved better inhibitors.

Chart 1. *C*-β-D-Glucopyranosyl heterocycles as inhibitors (K_i [µM]) of rabbit muscle glycogen phosphorylase *b* (rmGP*b*)

	1	2
	229^{25}	11^{25}
	76^{26}	9^{26}

R	phenyl (a)	naphthyl (b)
3 (1,2,4-oxadiazole)	$64^{27, 28}$	$12\ (2.4)^{28}$
4 (1,2,4-triazole)	$7^{29, 30}$	$0.41^{29, 30}$
(isoxazole)	no inh. at 625 µM^{31}	-

5

400[31]   -

6

310[31]   158[31]

7

0.28[31]   0.031[31]

8

Synthetic target compounds of this study

In this paper we disclose our studies on the preparation of several *C*-β-D-glucopyranosyl pyrrole and indole derivatives to answer the question if heterocycles with one HBD atom would make good inhibitors of GP, and present an improved synthesis of 2-(β-D-glucopyranosyl) imidazoles. In addition, the latter compounds have been tested against human liver GPa (hlGPa), the pharmaceutical target, and the crystal structure of rmGPb in complex with the most efficient compounds have been determined to elucidate the structural basis of their inhibitory potency.

Results and Discussion

Syntheses

For the preparation of *C*-glycosyl pyrroles a generally used method is the reaction of an electron rich pyrrole derivative with an electrophilic glycosyl donor. Typically, such reactions of 1*H*-pyrroles give 2-glycosylated products.[32-34] For the synthesis of the target compounds 2- (**11**)[35] and 3-arylpyrroles (**12a**,[36] **12b**[37]) were prepared according to previously reported methods. *C*-glycosylation of **10** and **11** with *O*-peracetylated β-D-glucopyranosyl-trichloroacetimidate[38] **9** in the presence of BF$_3$·OEt$_2$ furnished the β-configured ($^3J_{1',2'}$ > 9 Hz) products **13**[33] and **15**, respectively, in moderate to high yields as expected (Scheme 1). Surprisingly, glycosylation of 3-arylpyrroles **12** took place in the sterically more crowded 2-position to give **17**. The site of *C*-glucosylation in **15b** and **17b** was established by ^{1}H-^{1}H NOE experiments (Figure 1). In the NMR spectra of **15b** the characteristic resonances of H-3 (6.53 ppm, $J \approx$ 3 Hz), H-4 (6.24 ppm, $J \approx$ 3 Hz) and C-3 (106.6 ppm), C-4 (110.2 ppm) indicate the 2,5-disubstituted pyrrole structure,[39] and this is also proved by the observed NOEs. In case of **17b** the 2,3-disubstituted pyrrole could not be differentiated from a 2,4-disubstituted pyrrole by a simple analysis of ^{1}H (pyrrole-H resonances at 6.43 and 6.86 ppm $J \approx$ 2.6 Hz) and ^{13}C (pyrrole CH signals: 109.3, 119.2 ppm) spectra. However, NOE between H-4 and H-5 as well as the proximity of the sugar and naphthyl moieties (H-1'−naphthyl-H NOEs) indicate the 2,3-disubstitution of the pyrrole ring. *O*-Acetyl protecting groups were removed by the Zemplén protocol to obtain the test compounds **14**, **16**, and **18**.
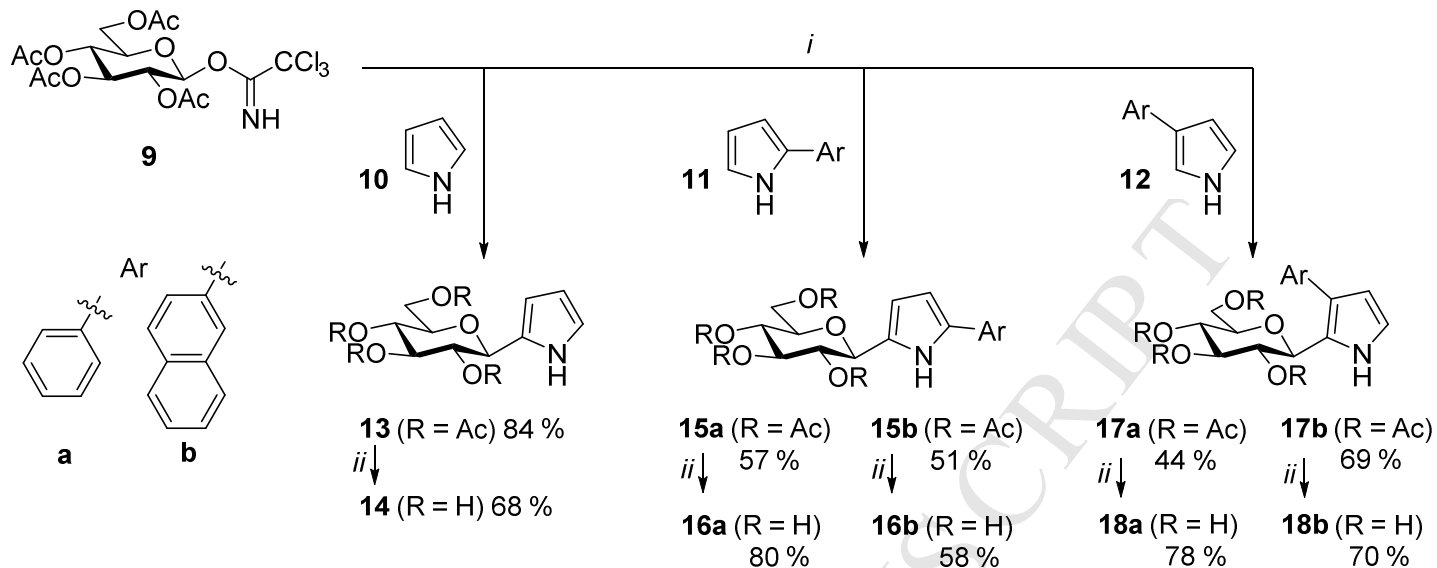
Scheme 1. Reaction conditions: *i*) BF$_3$·Et$_2$O, 4 Å molecular sieves, dry CH$_2$Cl$_2$, −50 °C to rt; *ii*) cat. NaOMe in MeOH, rt.
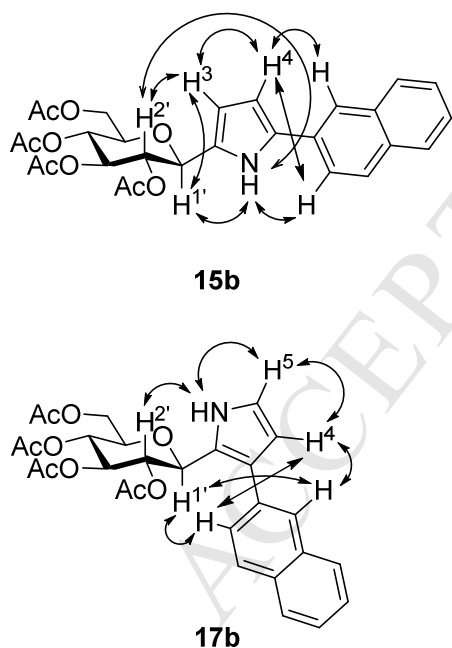
Figure 1. Nuclear Overhauser effects observed in *C*-glucopyranosylated (2-naphthyl)-pyrroles.

Synthesis of 2-glycosyl indoles was studied in detail in the course of the preparation of *C*-mannosyl tryptophan and analogous compounds.[40] 2-(β-D-Glucopyranosyl) indole (**23**) was prepared by adaptation and slight modification of the reported method. *O*-Perbenzylated glucosyl acetylene[41] **19** was cross-coupled with *N*-tosyl-2-iodoaniline (**20**) and cyclized to indole **21**[40] in one step. Subsequent detosylation with Bu₄NF and debenzylation by catalytic hydrogenolysis yielded the target 2-β-D-glucopyranosyl indole **23**.
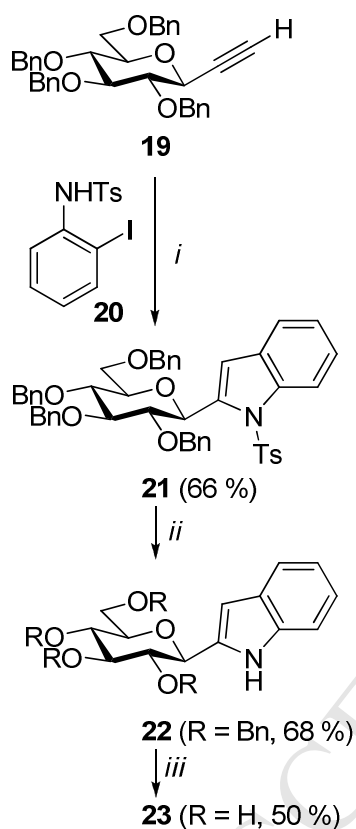
Scheme 2. Reaction conditions: *i*) Pd(PPh₃)₄, CuI, PPh₃, dry Et₃N, 75 °C, under Ar; *ii*) Bu₄NF, THF, reflux; *iii*) H₂ (10 bar), Pd(C), dry EtOAc, rt.

In a recent communication we presented the first preparation of 4(5)-aryl-2-(β-D-glucopyranosyl) imidazoles **8** (Chart 1) based on the cyclisation of *O*-perbenzoylated *C*-β-D-glucopyranosyl formamidine with α-bromoketones.[31] However, this transformation furnished the protected imidazoles **26** only in low yields (10-29 %). In order to find a more efficient procedure for the formation of **26** another ring-closing reaction was investigated: ethyl *C*-β-D-glucopyranosyl formimidate[42] (**24**) was treated with α-amino ketones **25** (obtained from the corresponding α-azido ketones as described in the supporting information) in anhydrous pyridine providing the desired imidazoles in satisfactory yields (Scheme 3).
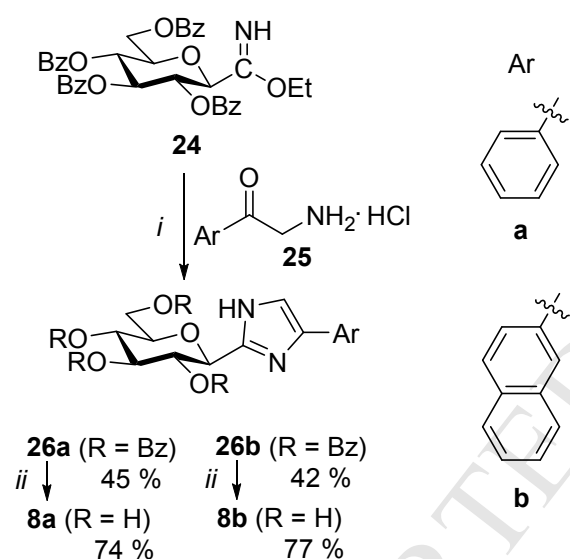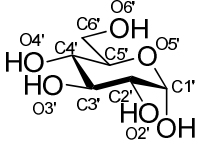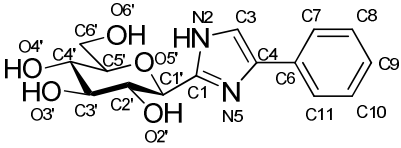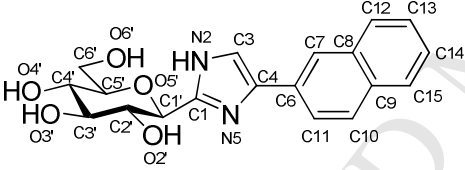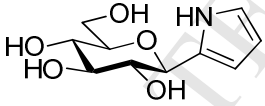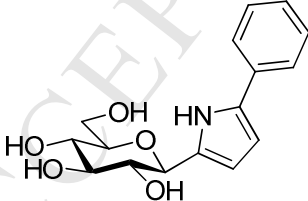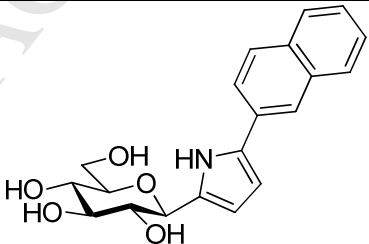
Scheme 3. Reaction conditions: *i*) dry pyridine, rt; *ii*) cat. NaOMe in MeOH, rt.
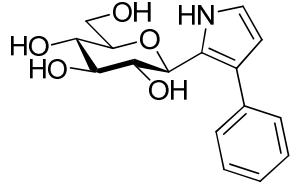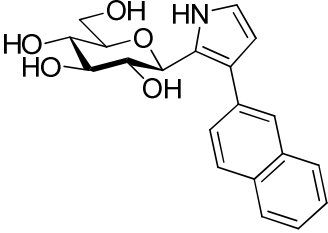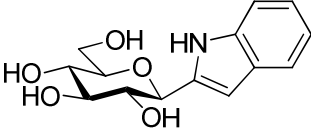
Kinetic Studies

The test compounds were evaluated against GPs of various origin and activation state and the data are collected in Table 1. The pyrrole derivatives **14**, **16**, **18**, and indole **23** were tested as inhibitors of rmGPb, the prototype of GPs,[43] by using an assay described previously.[44] The pyrroles **14**, **16**, and **18** proved inactive in the concentration range studied (the highest applied concentration was 625 μM) while indole **23** exhibited very weak inhibition, therefore, these compounds were not investigated further.

Since imidazoles **8** were shown to be the strongest glucose derived inhibitors of rmGPb known to date,[31] the inhibitory potency of **8a** and **8b** has been evaluated against hlGPa. For comparison purposes we also determined their potency with rmGPa and measured the inhibitory potency of α-D-glucose for hlGPa. Both compounds **8** are competitive inhibitors with respect to substrate Glc-1-P as revealed by the Lineweaver-Burk plots that intersect at the same point on the y-axis for hlGPa and rmGPa. The K_i values derived from the Dixon plots (1/v vs [I]) were for **8a** 0.156 μM and 0.226 μM for hlGPa and rmGPa, respectively. For **8b** they were found to be 0.026 μM and 0.065 μM for hlGPa and rmGPa, respectively. These values are in agreement with their respective inhibition constants for rmGPb[31] and indicate that **8a** and **8b** are approximately 27400 and 164600 times, respectively, more potent than α-D-glucose. They also indicate that the compound with the 2-naphthyl group is more efficient than its phenyl counterpart. Furthermore, it seems that the two compounds do not display any preference for the three isoenzymes (hlGPa, rmGPa and rmGPb) since they inhibit all three with similar potency.

Table 1. The chemical structures and the inhibition constants of the compounds studied. The crystallographic numbering scheme for the inhibitor atoms in D-glucose, **8a**, and **8b** is also shown.

Compound number	Chemical Structure	K_i (µM)		
		hlGPa	rmGPa	rmGPb
α-D-Glc		4280 ± 410	2000[45]	1700[46]
8a		0.156 ± 0.008	0.226 ± 0.098	0.280[31]
8b		0.026 ± 0.006	0.065 ± 0.003	0.031[31]
14		ND	ND	no inh. at 625 µM
16a		ND	ND	no inh. at 625 µM
16b		ND	ND	no inh. at 625 µM

18a		ND	ND	no inh. at 625 μM
18b		ND	ND	no inh. at 625 μM
23		ND	ND	IC$_{50}$ 625 μM

ND: not determined

Structural Studies

The crystal structures of rmGPb in complex with **8a** and **8b** have been determined at high resolution (1.85 Å). Both inhibitors were found bound at the catalytic site with all atoms well defined within the electron density map (Fig. 1). The binding of **8a** and **8b** does not trigger any significant conformational change to rmGPb and the r.m.s.d. between the complex structures and the ligand-free structure over well-defined residues gave a r.m.s.d. of 0.15 and 0.14 Å for Ca atoms for the **8a** and **8b** complexes, respectively. Upon binding both inhibitors displace four water molecules from the active site and they bind in similar structural mode (Fig. 2). The most characteristic feature is the anchoring of their β-D-glucopyranose moiety at the rmGPb glucose binding site and its interactions with protein residues (Table 2). These are essentially the same with those formed by glucose with rmGPb.[47] The imidazole linker engages in a hydrogen bond interaction with the main chain oxygen of His377 via N(H)2 and in

13

water mediated interactions with Asp283 side chain via N5. The interaction with the carbonyl oxygen of His377 has been previously observed for the amide nitrogen of *N*-acetyl-β-D-glucopyranosylamine (K_i = 32 μM),[48, 49] of glucopyranosylidene-spirohydantoin (K_i = 3.1 μM),[50, 51] and -thiohydantoin (K_i = 5.1 μM),[52] β-D-glucopyranosyl formamide analogs (K_i = 310 – 1800 μM),[53] and *C*-(β-D-glucopyranosyl)benzimidazole (K_i = 9 μM).[26] The increased inhibitory potency of these compounds was attributed to the interaction with the main chain oxygen of His377 and one of the design goals of **8** was to exploit this interaction. In addition, participation of heterocyclic nitrogen atoms in water mediated interactions were observed for C-β-D-glucopyranosyl benzimidazole[26] (**2**), 5-methyl-1,3,4-oxadiazole,[26, 28] and 5-(2-naphthyl)-1,2,4-oxadiazole[21] (**3b**) derivatives. In these compounds the nitrogen atoms are in the same position as N5 in the imidazoles. A comparison of the inhibitory efficiency of benzimidazole **2** (K_i = 9 μM) and indole **23** (IC_{50} ~ 625 μM) shows the practical loss of activity for the latter that may be explained by the absence of the second nitrogen in **23** (assuming that the heterocycle is oriented towards the formation of the H-bond to His377). The absence of this nitrogen in the pyrrole ring may also explain the loss of activity for pyrroles **16** and **18** in which the orientation of NH towards His377 places the aromatic residues into highly unfavourable positions. The opposite orientation allowing the participation of the ring N in water mediated interactions would result in the loss of the H-bonding ability to His377 and this, even if the position of the aromatic moieties would be optimal in **16**, seems detrimental for the binding.
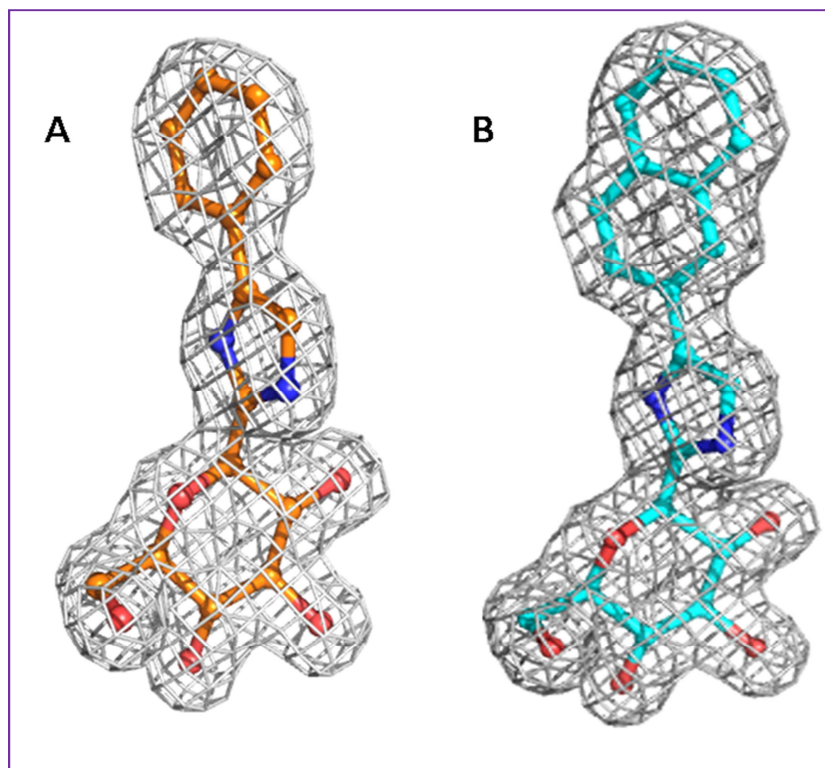
Figure 1. Diagram showing the electron density map of **8a** (A) and **8b** (B) before incorporating the atomic models of the inhibitors (presented as ball-and-stick-models).

Table 2. Hydrogen bond interactions of **8a**, and **8b** in the crystal. Numbers shown are distances in Å.

Inhibitor atom	Protein atom	8a	8b
O2'	Asn284 ND2	3.3	2.9
	Tyr573 OH	3.1	3.1
	Glu672 OE1	3.2	3.1
	Water	2.9	2.9
	Water	2.9	3.0
O3'	Glu672 OE1	2.8	2.7

	Ala673 N	3.3	3.3
	Ser674 N	3.1	3.1
	Gly675 N	3.2	3.1
O4'	Gly675 N	2.9	2.9
	Water	2.7	2.6
O6'	His377 ND1	2.7	2.7
	Asn484 ND2	2.8	2.8
N2	His377 O	2.9	2.9
N5	Water	2.8	2.8
Total		**15**	**15**

The phenyl and the naphthyl groups of **8a** and **8b**, respectively, bind at the β-cavity engaging in numerous van der Waals interactions. Both phenyl and naphthyl are involved in 18 van der Waals interactions with Glu88 (1), Asn282 (2), Asn284 (8), Phe285 (2), and His341 (5). In addition, the naphthyl group is involved in 11 van der Waals interactions with Asn282 (1), Phe285 (3), Phe286 (1), Arg292 (2), His341 (3), and Ala383 (1). The structural basis of the inhibitory potency of the two compounds seems to lie on their interactions with the side chains of Asn282, Asp283, and Asp284 which hold the 280s loop in its closed T-state conformation, therefore inhibiting access of the substrate to the catalytic site. The additional van der Waals interactions of **8b** seem to form the structural basis for the significant difference in the inhibitory potencies of these two inhibitors.

16
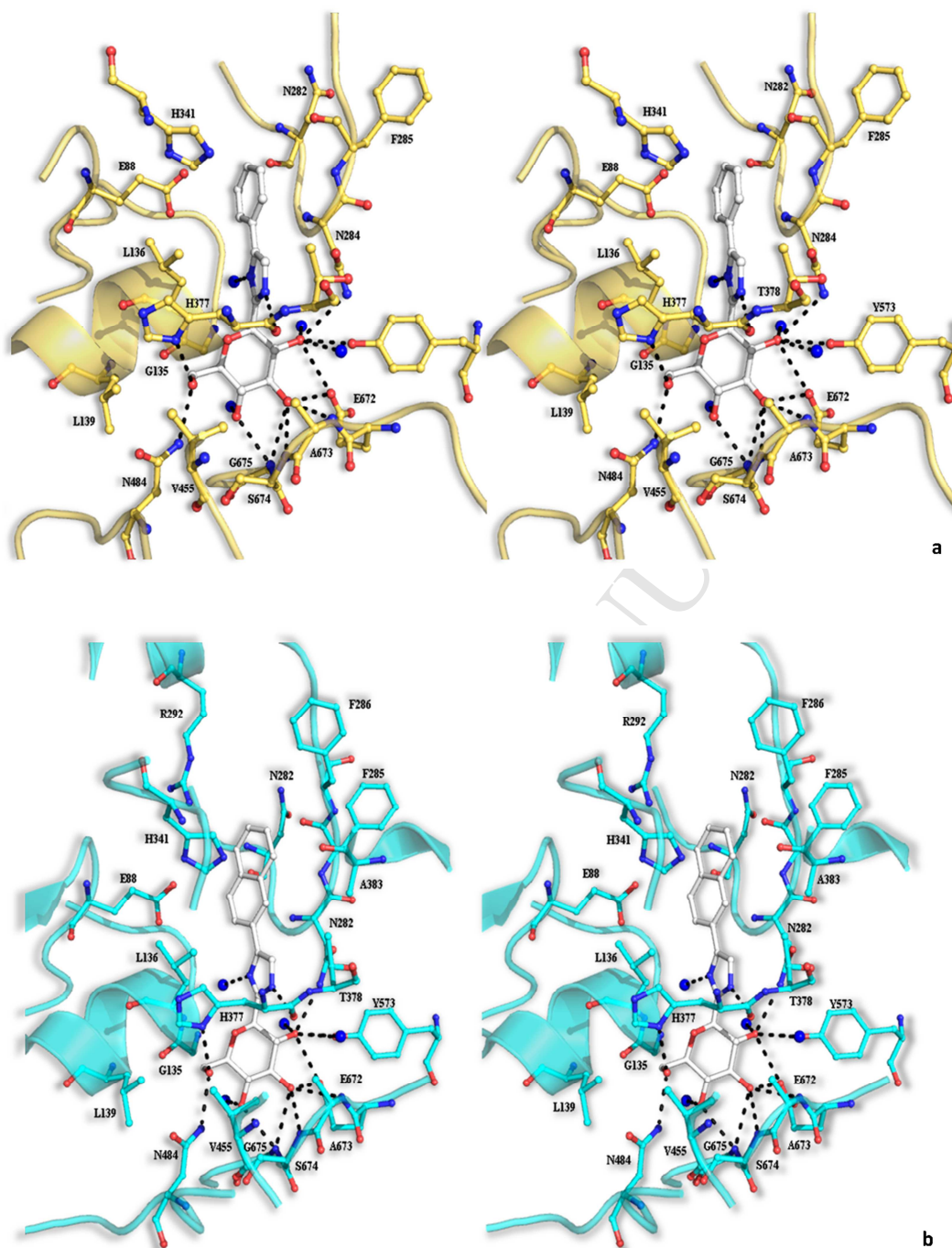
Figure 2. Stereo diagram showing the network of interactions formed between **8a** (a) and **8b** (b) with residues at active site of rmGPb. Hydrogen bond interactions are represented as dotted lines and water molecules as blue spheres.

Conclusion

Syntheses of a series of *C*-glucopyranosyl pyrroles, indole, and an improved preparation of C-glucopyranosyl imidazoles allowed us to study and compare their inhibitory efficiency against isoforms of GP. While pyrroles had no effect with rmGPb, imidazoles proved to be the best known glucose analogue inhibitors of rmGPb, rmGPa, and also of hlGPa, the physiologically relevant enzyme. Structural investigations of the rmGPb-imidazole complexes by X-ray crystallography revealed important interactions between the imidazole ring and the protein, such as the H-bridge from N(H)2 to His377 and involvement of N5 in water mediated H-bond networks. The absence of the latter interactions in the pyrroles may explain why these compounds show no inhibitory activity.

Experimental

Syntheses

General methods

Melting points were measured on a Kofler hot-stage and are uncorrected. Optical rotations were determined with a Perkin-Elmer 241 polarimeter at rt. NMR spectra were recorded with Bruker 360 (360/90 MHz for ^{1}H/^{13}C) or Bruker Avance II 500 (500.13/125.76 for ^{1}H/^{13}C) spectrometers. Chemical shifts are referenced to Me$_4$Si (^{1}H), or to the residual solvent signals (^{13}C). Mass spectra were recorded with a Thermo LTQ XL mass spectrometer (Thermo Electron Corp., San Jose, CA, USA) operated in a full scan positive ion ESI mode. Microanalyses were performed on an Elementar Vario Micro cube

instrument. TLC was performed on DC-Alurolle Kieselgel 60 F_{254} (Merck) plates, visualized under UV light and by gentle heating. For column chromatography Kieselgel 60 (Merck, particle size 0.063-0.200 mm) was used. EtOAc (P_4O_{10}), CH_2Cl_2 (P_4O_{10}) and Et_3N (CaH_2) were distilled from the given drying agents and stored over 4 Å molecular sieves. MeOH was purified by distillation after refluxing for a couple of hours with magnesium turnings and iodine. Pyridine (VWR), pyrrole, tetrakis(triphenylphosphine)palladium(0), TOSMIC, 2-vinylnaphthalene (Sigma-Aldrich) were purchased from the indicated suppliers. 2,3,4,6-Tetra-*O*-acetyl-β-D-glucopyranosyl-trichloroacetimidate[38] (**9**), the 2-aryl-1*H*-pyrroles[35] (**11a,b**), the 3-aryl-1*H*-pyrroles (**12a**,[36] **12b**[37]), 2,3,4,6-tetra-*O*-benzyl-β-D-glucopyranosyl-ethyne[41] (**19**), *N*-tosyl-2-iodoaniline[54] (**20**), ethyl *C*-(2,3,4,6-tetra-*O*-benzoyl-β-D-glucopyranosyl)formimidate[42] (**24**) and the 2-azido-1-arylethanones[55] were synthesized according to published procedures.

General procedures

General procedure I for the synthesis of 2-(2',3',4',6'-tetra-O-acetyl-β-D-glucopyranosyl)-pyrroles (13, 15, 17)

2,3,4,6-Tetra-*O*-acetyl-β-D-glucopyranosyl-trichloroacetimidate (**9**, 100 mg, 0.2 mmol) and pyrrole (**10**, 1 mmol) or the corresponding aryl-pyrrole (**11a,b** or **12a,b**, 0.2 mmol) were dissolved in anhydrous CH_2Cl_2 (3 ml) and activated 4 Å molecular sieves (powder, 200 mg) were added. The mixture was cooled to −50 °C and $BF_3 \cdot Et_2O$ (12 μl, 0.1 mmol) was added dropwise with continuous stirring. The reaction was stirred for 1h at −50 °C, then slowly allowed to reach room temperature and stirred for the given time. After total consumption of the trichloroacetimidate (judged by TLC, 1:1 hexane-EtOAc), molecular sieves were removed by filtration and the filtrate was purified by column chromatography.

General procedure II for the preparation of 2-amino-1-arylethanone hydrochlorides (25)

To a degassed solution of a 2-azido-1-arylethanone (18.6 mmol) in methanol (100 mL) a solution of tin(II) chloride dihydrate (12.65 g, 55.8 mmol) in methanol (160 mL) was added and the mixture was stirred at rt under N_2 atmosphere. When the TLC (3:1 hexane-EtOAc) showed total consumption of the starting material (5-24 h) dry HCl gas was bubbled through the reaction mixture over 12 h. The solution was then concentrated under reduced pressure and the residue was put into the freezer for overnight. The resulting precipitates were filtered off and washed with cold methanol. The products were used in the next step without further purification.

General procedure III for the synthesis of 4(5)-aryl-2-(2',3',4',6'-tetra-O-benzoyl-β-D-glucopyranosyl)-imidazoles (26)

Ethyl *C*-(2,3,4,6-tetra-*O*-benzoyl-β-D-glucopyranosyl)formimidate (**24**, 0.15 mmol) and the corresponding 2-amino-1-arylethanone hydrochloride (**25**, 0.31 mmol, 2 equiv.) were dissolved in anhydrous pyridine (4 mL) and the reaction mixture was stirred at rt. After completion of the reaction (1-2 d) monitored by TLC (3:2 hexane-EtOAc) the solvent was removed under diminished pressure and the residue was purified by column chromatography.

General procedure IV for removal of the O-acetyl protecting groups (for the preparation of test compounds 14, 16, 18)

An *O*-acetyl protected compound (100 mg) was dissolved in anh. MeOH (5 mL), a few drops of ~1M solution of NaOMe in MeOH was added and the mixture was left to stand at rt. After complete conversion (judged by TLC, 7:3 $CHCl_3$-MeOH) the reaction mixture was neutralized by the careful addition of AcOH and evaporated in vacuo. The crude product was purified by column chromatography.

Protein production and purification

Rabbit skeletal muscle glycogen phosphorylase b (rmGPb) was isolated, and purified as described previously.[56] RmGPa was prepared from rmGPb by phosphorylation with a truncated form of the γ (catalytic) subunit of rabbit skeletal muscle phosphorylase kinase produced as described previously.[57] Human liver glycogen phosphorylase a (hlGPa) was expressed from the pET160DEST vector (Invitrogen) with a His tag (6x) followed by the Lumio tag and a TEV protease prescission site in *E.coli* strain BL21 Gold (DE3) (Agilent Technologies). The strain was inoculated in LB medium (plus 50 μg/mL ampicillin, 100 mg/L pyridoxine, and 600 mg/L $MnCl_2$) grown at 37 °C to a cell density of OD_{600}= 0.7 and induced for 15 hr with 0.6 mM isopropyl-1-thio-β-D-galactoside (IPTG) prior to harvest. The *E. coli* cells were resuspended in lysis buffer (50 mM Na_2HPO_4/NaH_2PO_4 [pH 8.0], containing 500 mM NaCl, 20 mM imidazole, a Protease inhibitor cocktail tablet (EDTA-free, Roche) and 50 U Benzonase) and sonicated at 4° C. The lysate was clarified by centrifugation at 16,000 × g for 1 hr. hlGPb in the soluble fraction of the lysate was purified using a Ni^{2+} Sepharose chromatography. His-tag tail was removed by cleaving with TEV protease and Ni^{2+} Sepharose chromatography. A final step using anion-exchange chromatography led to a pure hlGPb sample as judged by the appearance of a single band in SDS page.Phosphorylation to hlGPa was performed using a truncated form of the γ (catalytic) subunit of rabbit skeletal muscle phosphorylase kinase.

Kinetic studies

Kinetic studies with hlGPa were performed at 30° C in the direction of glycogen synthesis by measuring the inorganic phosphate released in the reaction.[56] Briefly, the enzyme (5 μg/ml rmGPb or rmGPa, and 1

µg/mL hlGPa) was assayed in a 30 mM imidazole/HCl buffer (pH 6.8) containing 60 mM KCl, 0.6 mM

EDTA, and 0.6 mM dithiothreitol using constant concentrations of glycogen (0.2% w/v), AMP (1 mM;

only for the rmGPb experiments), and various concentrations of Glc-1-P and inhibitors. For the

measurement of the K_i for α-D-glucose for hlGPa solutions of four different concentrations were used 2

min after dissolution while the overall assay time was 1 minute following a previously described

method.[46] Initial velocities were calculated from the pseudo-first order rate constants. Kinetic data

presented in the form of Lineweaver-Burk, or Dixon plots were analysed for the calculation of the kinetic

parameters by the non-linear regression program GRAFIT.[58]

X-ray crystallography

Tetragonal T state rmGPb crystals were grown as described previously.[59] These crystals belong to space

group $P4_32_12$ with unit cell dimensions a=b=128.6 Å and c=116.3 Å. rmGPb – inhibitor complexes were

formed by diffusion of a 10 mM solution of the inhibitor in the crystallization media (supplemented with

15% (v/v) DMSO) in preformed rmGPb crystals at room temperature for 6 hours prior to data collection.

X-ray diffraction data were collected using synchrotron radiation on station ID911-2 at MAX-Lab

Synchrotron Radiation Source in Lund, Sweden. Crystal orientation, integration of reflections, inter-

frame scaling, partial reflection summation, and data reduction was performed by the program

Mosflm.[60] Scaling and merging of intensities were performed by SCALA.[61] Crystallographic refinement of

the complexes was performed by maximum-likelihood methods using REFMAC.[61] The starting model

employed for the refinement of the complexes was the structure of the native T state rmGPb complex

determined at 1.9 Å resolution (Leonidas et al., unpublished results). Ligand molecule coordinates and

topologies were constructed using JLigand[62] and they were fitted to the electron density maps after

adjustment of their torsion angles. Alternate cycles of manual rebuilding with the molecular graphic

program COOT[61] and refinement with REFMAC[63] improved the quality of the models. A summary of the data processing and refinement statistics for the inhibitor complex structures is given in Table 2. The stereochemistry of the protein residues was validated by MolProbity.[64] Hydrogen bonds and van der Waals interactions were calculated with the program CONTACT as implemented in CCP4[61] applying a distance cut off 3.3 Å and 4.0 Å, respectively. Figures were prepared with PyMol.[65] The coordinates of the new structures have been deposited with the RCSB Protein Data Bank (http://www.rcsb.org/pdb) with codes presented in Table 3.

Table 3. Summary of the diffraction data processing and refinement statistics for the rmGPb complexes. Values in parentheses are for the outermost shell.

GPb complex	**8a**	**8b**
Data collection and processing statistics		
Resolution (Å)	38.39 – 1.85	38.76 – 1.85
Outermost shell (Å)	1.95 – 1.85	1.95 – 1.85
Reflections measured	323721 (46061)	326554 (46626)
Unique reflections	82598 (11847)	74394 (11353)
Multiplicity	3.9 (3.9)	4.4 (4.1)
R_{symm}	0.069 (0.428)	0.111 (0.450)
Completeness (%)	99.3 (98.7)	89.9 (94.8)

<I/σI >	12.2 (3.3)	4.9 (2.6)
Refinement statistics		
R_{cryst}	0.158 (0.240)	0.170 (0.240)
R_{free}	0.188 (0.260)	0.203 (0.286)
No of solvent molecules	321	324
r.m.s. deviation from ideality		
in bond lengths (Å)	0.01	0.01
in angles (°)	1.3	1.3
Average B factor ($Å^2$)		
Protein atoms	30.7	29.8
Solvent molecules	36.9	36.1
Inhibitor atoms	18.0	17.4
PDB entry	5JTT	5JTU

Acknowledgments

Supporting information

Detailed description of synthetic procedures and compound characterization, copies of NMR spectra of the new compounds.

References

1.   Oikonomakos, N. G. Glycogen phosphorylase as a molecular target for type 2 diabetes therapy. *Curr. Protein Pept. Sci.* **2002,** 3, 561-586.

2.   Barford, D.; Johnson, L. N. The Allosteric Transition of Glycogen-Phosphorylase. *Nature* **1989,** 340, 609-616.

3.   Barford, D.; Hu, S. H.; Johnson, L. N. Structural Mechanism for Glycogen-Phosphorylase Control by Phosphorylation and AMP. *J. Mol. Biol.* **1991,** 218, 233-260.

4.   Somsák, L.; Czifrák, K.; Tóth, M.; Bokor, É.; Chrysina, E. D.; Alexacou, K. M.; Hayes, J. M.; Tiraidis, C.; Lazoura, E.; Leonidas, D. D.; Zographos, S. E.; Oikonomakos, N. G. New inhibitors of glycogen phosphorylase as potential antidiabetic agents. *Curr. Med. Chem.* **2008,** 15, 2933-2983.

5.   Hayes, J.; Kantsadi, A.; Leonidas, D. Natural products and their derivatives as inhibitors of glycogen phosphorylase: potential treatment for type 2 diabetes. *Phytochem. Rev.* **2014,** 13, 471-498.

6.   Rath, V. L.; Ammirati, M.; Danley, D. E.; Ekstrom, J. L.; Gibbs, E. M.; Hynes, T. R.; Mathiowetz, A. M.; McPherson, R. K.; Olson, T. V.; Treadway, J. L.; Hoover, D. J. Human liver glycogen phosphorylase inhibitors bind at a new allosteric site. *Chem. Biol.* **2000,** 7, 677-682.

7.   Agius, L. Physiological Control of Liver Glycogen Metabolism: Lessons from Novel Glycogen Phosphorylase Inhibitors. *Mini-Rev. Med. Chem.* **2010,** 10, 1175-1187.

8.   Kurukulasuriya, R.; Link, J. T.; Madar, D. J.; Pei, Z.; Richards, S. J.; Rohde, J. J.; Souers, A. J.; Szczepankiewicz, B. G. Potential drug targets and progress towards pharmacologic inhibition of hepatic glucose production. *Curr. Med. Chem.* **2003,** 10, 123-153.

9.   Agius, L. New hepatic targets for glycaemic control in diabetes. *Best Pract. Res. Clin. Endocrin. Metab.* **2007,** 21, 587-605.

10.   Treadway, J. L.; Mendys, P.; Hoover, D. J. Glycogen phosphorylase inhibitors for treatment of type 2 diabetes mellitus. *Expert Opin. Invest. Drugs* **2001,** 10, 439-454.

11.   Tracey, W. R.; Treadway, J. L.; Magee, W. P.; Sutt, J. C.; McPherson, R. K.; Levy, C. B.; Wilder, D. E.; Yu, L. J.; Chen, Y.; Shanker, R. M.; Mutchler, A. K.; Smith, A. H.; Flynn, D. M.; Knight, D. R.

Cardioprotective effects of ingliforib, a novel glycogen phosphorylase inhibitor. *Am. J. Physiol.-Heart Circul. Physiol.* **2004,** 286, H1177-H1184.

12.   Treadway, J. L.; Magee, W. P.; Hoover, D. J.; McPherson, R. K.; Martin, W. H.; Zavadoski, W. J.; Gibbs, E. M.; Tracey, W. R. Cardioprotective effect of the glycogen phosphorylase inhibitor CP-380867. *Diabetes* **2000,** 49, A127-A127.

13.   Favaro, E.; Bensaad, K.; Chong, M. G.; Tennant, D. A.; Ferguson, D. J. P.; Snell, C.; Steers, G.; Turley, H.; Li, J.-L.; Günther, U. L.; Buffa, F. M.; McIntyre, A.; Harris, A. L. Glucose Utilization via Glycogen Phosphorylase Sustains Proliferation and Prevents Premature Senescence in Cancer Cells. *Cell Metab.* **2012,** 16, 751-764.

14.   Zois, C. E.; Favaro, E.; Harris, A. L. Glycogen metabolism in cancer. *Biochem. Pharmacol.* **2014,** 92, 3-11.

15.   Lew, C. R.; Guin, S.; Theodorescu, D. Targeting glycogen metabolism in bladder cancer. *Nat. Rev. Urol.* **2015,** 12, 383-391.

16.   Zois, C. E.; Harris, A. L. Glycogen metabolism has a key role in the cancer microenvironment and provides new targets for cancer therapy. *J. Mol. Med.* **2016,** 94, 137-154.

17.   Xu, L.; Sun, H. Pharmacological manipulation of brain glycogenolysis as a therapeutic approach to cerebral ischemia. *Mini Rev Med Chem* **2010,** 10, 1188-93.

18.   Guan, T.; Qian, Y. S.; Tang, X. Z.; Huang, M. H.; Huang, L. F.; Li, Y. M.; Sun, H. B. Maslinic Acid, a Natural Inhibitor of Glycogen Phosphorylase, Reduces Cerebral Ischemic Injury in Hyperglycemic Rats by GLT-1 Up-Regulation. *J. Neurosci. Res.* **2011,** 89, 1829-1839.

19.   Somsák, L. Glucose derived inhibitors of glycogen phosphorylase. *Compt. Rend. Chimie* **2011,** 14, 211-223.

20.   Somsák, L.; Nagy, V.; Hadady, Z.; Docsa, T.; Gergely, P. Glucose analog inhibitors of glycogen phosphorylases as potential antidiabetic agents: recent developments. *Curr. Pharma. Design* **2003,** 9, 1177-1189.

21.   Oikonomakos, N. G.; Somsák, L. Recent advances in glycogen phosphorylase inhibitor design. *Curr. Opin. Invest. Drugs* **2008,** 9, 379-395.

22.   Somsák, L.; Nagy, V.; Hadady, Z.; Felföldi, N.; Docsa, T.; Gergely, P. Recent developments in the synthesis and evaluation of glucose analog inhibitors of glycogen phosphorylases as potential antidiabetic agents. In *Frontiers in Medicinal Chemistry*, Reitz, A. B.; Kordik, C. P.; Choudhary, M. I.; Rahman, A. u., Eds. Bentham: 2005; Vol. 2, pp 253-272.

23.   Hayes, J. M.; Kantsadi, A. L.; Leonidas, D. D. Natural products and their derivatives as inhibitors of glycogen phosphorylase: potential treatment for type 2 diabetes. *Phytochem. Rev.* **2014,** 13, 471-498.

24.   Praly, J. P.; Vidal, S. Inhibition of Glycogen Phosphorylase in the Context of Type 2 Diabetes, with Focus on Recent Inhibitors Bound at the Active Site *Mini-Rev. Med. Chem.* **2010,** 10, 1102-1126.

25.   Hadady, Z.; Tóth, M.; Somsák, L. *C*-(β-D-glucopyranosyl) heterocycles as potential glycogen phosphorylase inhibitors. *Arkivoc* **2004,** (vii), 140-149.

26.   Chrysina, E. D.; Kosmopolou, M. N.; Tiraidis, C.; Kardarakis, R.; Bischler, N.; Leonidas, D. D.; Hadady, Z.; Somsák, L.; Docsa, T.; Gergely, P.; Oikonomakos, N. G. Kinetic and crystallographic studies on 2-(β-D-glucopyranosyl)-5-methyl-1,3,4-oxadiazole, -benzothiazole, and -benzimidazole, inhibitors of muscle glycogen phosphorylase *b*. Evidence for a new binding site. *Protein Sci.* **2005,** 14, 873-888.

27.   Benltifa, M.; Vidal, S.; Fenet, B.; Msaddek, M.; Goekjian, P. G.; Praly, J.-P.; Brunyánszki, A.; Docsa, T.; Gergely, P. In the Search of Glycogen Phosphorylase Inhibitors: 5-Substituted 3-*C*-Glucopyranosyl-1,2,4-Oxadiazoles from β-D-Glucopyranosyl Cyanides upon Cyclization of *O*-Acyl-amidoxime Intermediates. *Eur. J. Org. Chem.* **2006**, 4242-4256.

28.	Tóth, M.; Kun, S.; Bokor, É.; Benltifa, M.; Tallec, G.; Vidal, S.; Docsa, T.; Gergely, P.; Somsák, L.; Praly, J.-P. Synthesis and structure-activity relationships of *C*-glycosylated oxadiazoles as inhibitors of glycogen phosphorylase. *Bioorg. Med. Chem.* **2009,** 17, 4773-4785.

29.	Bokor, É.; Docsa, T.; Gergely, P.; Somsák, L. *C*-Glucopyranosyl-1,2,4-triazoles as new potent inhibitors of glycogen phosphorylase. *ACS Med. Chem. Lett.* **2013,** 4, 612-615.

30.	Kun, S.; Bokor, É.; Varga, G.; Szőcs, B.; Páhi, A.; Czifrák, K.; Tóth, M.; Juhász, L.; Docsa, T.; Gergely, P.; Somsák, L. New synthesis of 3-(β-D-glucopyranosyl)-5-substituted-1,2,4-triazoles, nanomolar inhibitors of glycogen phosphorylase. *Eur. J. Med. Chem.* **2014,** 76, 567-579.

31.	Bokor, É.; Kun, S.; Docsa, T.; Gergely, P.; Somsák, L. 4(5)-Aryl-2-C-glucopyranosyl-imidazoles as new nanomolar glucose analog inhibitors of glycogen phosphorylase. *ACS Med. Chem. Lett.* **2015,** 6, 1215-1219.

32.	Mukherjee, D.; Sarkar, S. K.; Chowdhury, U. S.; Taneja, S. C. A rapid stereoselective C-glycosidation of indoles and pyrrole via indium trichloride promoted reactions of glycosyl halides. *Tetrahedron Lett.* **2007,** 48, 663-667.

33.	Armitt, D. J.; Banwell, M. G.; Freeman, C.; Parish, C. R. C-Glycoside formation via Lewis acid promoted reaction of O-glycosylimidates with pyrroles. *J. Chem. Soc.-Perkin Trans. 1* **2002**, 1743-1745.

34.	Tram, K.; MacIntosh, W.; Yan, H. Synthesis of glycosyl dipyrromethanes. *Tetrahedron Lett.* **2009,** 50, 2278-2280.

35.	Rieth, R. D.; Mankad, N. P.; Calimano, E.; Sadighi, J. P. Palladium-catalyzed cross-coupling of pyrrole anions with aryl chlorides, bromides, and iodides. *Org. Lett.* **2004,** 6, 3981-3983.

36.	Smith, N. D.; Huang, D. H.; Cosford, N. D. P. One-step synthesis of 3-aryl- and 3,4-diaryl-(1H)-pyrroles using tosylmethyl isocyanide (TOSMIC). *Org. Lett.* **2002,** 4, 3537-3539.

37.	Pavri, N. P.; Trudell, M. L. An efficient method for the synthesis of 3-arylpyrroles *J. Org. Chem.* **1997,** 62, 2649-2651.

38.   Schmidt, R. R.; Jung, K. H. Oligosaccharide synthesis with trichloroacetimidate. In *Preparative carbohydrate chemistry*, Hanessian, S., Ed. Marcel Dekker, Inc.: 1997; p 296.

39.   Bird, C. W.; Cheeseman, G. W. H. Structure of Five-membered Rings with One Heteroatom. . In *Comprehensive Heterocyclic Chemistry*, Katritzky, A. R.; Rees, C. W., Eds. Pergamon: Oxford, 1984; pp 1-38.

40.   Nishikawa, T.; Koide, Y.; Kanakubo, A.; Yoshimura, H.; Isobe, M. Synthesis of beta-analogues of C-mannosyltryptophan, a novel C-glycosylamino acid found in proteins. *Org. Biomol. Chem.* **2006,** 4, 1268-1277.

41.   Dondoni, A.; Mariotti, G.; Marra, A. Synthesis of α- and β-Glycosyl Asparagine Ethylene Isosteres (C-Glycosyl Asparagines) via Sugar Acetylenes and Garner Aldehyde Coupling. *J. Org. Chem.* **2002,** 67, 4475-4486.

42.   Bokor, É.; Szilágyi, E.; Docsa, T.; Gergely, P.; Somsák, L. Synthesis of substituted 2-(β-D-glucopyranosyl)-benzimidazoles and their evaluation as inhibitors of glycogen phosphorylase. *Carbohydr. Res.* **2013,** 381, 179-186.

43.   Chrysina, E. D. The Prototype of Glycogen Phosphorylase *Mini-Rev. Med. Chem.* **2010,** 10, 1093-1101.

44.   Somsák, L.; Kovács, L.; Tóth, M.; Ősz, E.; Szilágyi, L.; Györgydeák, Z.; Dinya, Z.; Docsa, T.; Tóth, B.; Gergely, P. Synthesis of and a Comparative Study on the Inhibition of Muscle and Liver Glycogen Phosphorylases by Epimeric Pairs of D-Gluco- and D-Xylopyranosylidene-spiro-(thio)hydantoins and N-(D-Glucopyranosyl) Amides. *J. Med. Chem.* **2001,** 44, 2843-2848.

45.   Sprang, S. R.; Goldsmith, E. J.; Fletterick, R. J.; Withers, S. G.; Madsen, N. B. Catalytic Site of Glycogen Phosphorylase: Structure of the T State and Secificity for α-D-Glucose. *Biochem.* **1982,** 21, 5364-5371.

46.   Martin, J. L.; Veluraja, K.; Ross, K.; Johnson, L. N.; Fleet, G. W. J.; Ramsden, N. G.; Bruce, I.; Orchard, M. G.; Oikonomakos, N. G.; Papageorgiou, A. C.; Leonidas, D. D.; Tsitoura, H. S. Glucose Analogue Inhibitors of Glycogen Phosphorylase: The Design of Potential Drugs for Diabetes. *Biochem.* **1991,** 30, 10101-10116.

47.   Martin, J. L.; Johnson, L. N.; Withers, S. G. Comparison of the Binding of Glucose and Glucose 1-Phosphate Derivatives to T-State Glycogen Phosphorylase b. *Biochem.* **1990,** 29, 10745-10757.

48.   Oikonomakos, N. G.; Kontou, M.; Zographos, S. E.; Watson, K. A.; Johnson, L. N.; Bichard, C. J. F.; Fleet, G. W. J.; Acharya, K. R. N-Acetyl-beta-D-glucopyranosylamine: A potent T-state inhibitor of glycogen phosphorylase. A comparison with alpha-D-glucose. *Protein Sci.* **1995,** 4, 2469-2477.

49.   Watson, K. A.; Mitchell, E. P.; Johnson, L. N.; Cruciani, G.; Son, J. C.; Bichard, C. J. F.; Fleet, G. W. J.; Oikonomakos, N. G.; Kontou, M.; Zographos, S. E. Glucose Analogue Inhibitors of Glycogen Phosphorylase: from Crystallographic Analysis to Drug Prediction using GRID Force-Field and GOLPE Variable Selection. *Acta Cryst.* **1995,** D51, 458-472.

50.   Bichard, C. J. F.; Mitchell, E. P.; Wormald, M. R.; Watson, K. A.; Johnson, L. N.; Zographos, S. E.; Koutra, D. D.; Oikonomakos, N. G.; Fleet, G. W. J. Potent Inhibition of Glycogen Phosphorylase by a Spirohydantoin of Glucopyranose: First Pyranose Analogues of Hydantocidin. *Tetrahedron Lett.* **1995,** 36, 2145-2148.

51.   Gregoriou, M.; Noble, M. E. M.; Watson, K. A.; Garman, E. F.; Krülle, T. M.; Fuente, C.; Fleet, G. W. J.; Oikonomakos, N. G.; Johnson, L. N. The structure of a glycogen phosphorylase glucopyranose spirohydantoin complex at 1.8 A resolution and 100 K: The role of the water structure and its contribution to the binding. *Protein Sci.* **1998,** 7, 915-927.

52.   Oikonomakos, N. G.; Skamnaki, V. T.; Ősz, E.; Szilágyi, L.; Somsák, L.; Docsa, T.; Tóth, B.; Gergely, P. Kinetic and crystallographic studies of glucopyranosylidene spirothiohydantoin binding to glycogen phosphorylase b. *Bioorg. Med. Chem.* **2002,** 10, 261-268.

53.   Chrysina, E. D.; Oikonomakos, N. G.; Zographos, S. E.; Kosmopoulou, M. N.; Bischler, N.; Leonidas, D. D.; Kovács, L.; Docsa, T.; Gergely, P.; Somsák, L. Crystallographic studies on alpha- and beta-D-glucopyranosyl formamide analogues, inhibitors of glycogen phosphorylase. *Biocatal. Biotransform.* **2003,** 21, 233-242.

54.   Mailyan, A. K.; Geraskin, I. M.; Nemykin, V. N.; Zhdankin, V. V. Preparation, X-ray Structure, and Oxidative Reactivity of N-(2-Iodylphenyl)tosylamides and 2-Iodylphenyl Tosylate: Iodylarenes Stabilized by Ortho-Substitution with a Sulfonyl Group. *J. Org. Chem.* **2009,** 74, 8444-8447.

55.   Patonay, T.; Juhász-Tóth, É.; Bényei, A. Base-induced coupling of alpha-azido ketones with aldehydes - An easy and efficient route to trifunctionalized synthons 2-azido-3-hydroxy ketones, 2-acylaziridines, and 2-acylspiroaziridines. *Eur. J. Org. Chem.* **2002**, 285-295.

56.   Tsirkone, V. G.; Tsoukala, E.; Lamprakis, C.; Manta, S.; Hayes, J. M.; Skamnaki, V. T.; Drakou, C.; Zographos, S. E.; Komiotis, D.; Leonidas, D. D. 1-(3-Deoxy-3-fluoro-beta-D-glucopyranosyl) pyrimidine derivatives as inhibitors of glycogen phosphorylase b: Kinetic, crystallographic and modelling studies. *Bioorg. Med. Chem.* **2010,** 18, 3413-3425.

57.   Hayes, J. M.; Skamnaki, V. T.; Archontis, G.; Lamprakis, C.; Sarrou, J.; Bischler, N.; Skaltsounis, A. L.; Zographos, S. E.; Oikonomakos, N. G. Kinetics, in silico docking, molecular dynamics, and MM-GBSA binding studies on prototype indirubins, KT5720, and staurosporine as phosphorylase kinase ATP-binding site inhibitors: the role of water molecules examined. *Proteins* **2011,** 79, 703-19.

58.   Leatherbarrow, R. J. GraFit version 4.06. *Erithacus Software Ltd. Staines, U.K.* **1998**.

59.   Alexacou, K. M.; Tenchiu, A. C.; Chrysina, E. D.; Charavgi, M. D.; Kostas, I. D.; Zographos, S. E.; Oikonomakos, N. G.; Leonidas, D. D. The binding of β-D-glucopyranosyl-thiosemicarbazone derivatives to glycogen phosphorylase: A new class of inhibitors. *Bioorg. Med. Chem.* **2010,** 18, 7911-7922.

60.   Leslie, A. G. W.; Powell, H. R. Processing Diffraction Data with Mosflm. In *Evolving Methods for Macromolecular Crystallography*, Read, R. J.; Sussman, J. I., Eds. Springer: 2007; Vol. 245, pp 41-51.

61.   CCP4. The CCP4 suite : programs for protein crystallography. *Acta Crystallogr.* **1994,** D 50, 760-763.

62.   Lebedev, A. A.; Young, P.; Isupov, M. N.; Moroz, O. V.; Vagin, A. A.; Murshudov, G. N. JLigand: a graphical tool for the CCP4 template-restraint library. *Acta Crystallogr. D Biol. Crystallogr.* **2012,** 68, 431-40.

63.   Murshudov, G. N.; Skubak, P.; Lebedev, A. A.; Pannu, N. S.; Steiner, R. A.; Nicholls, R. A.; Winn, M. D.; Long, F.; Vagin, A. A. REFMAC5 for the refinement of macromolecular crystal structures. *Acta Crystallogr. D Biol. Crystallogr.* **2011,** 67, 355-67.

64.   Chen, V. B.; Arendall, W. B., 3rd; Headd, J. J.; Keedy, D. A.; Immormino, R. M.; Kapral, G. J.; Murray, L. W.; Richardson, J. S.; Richardson, D. C. MolProbity: all-atom structure validation for macromolecular crystallography. *Acta Crystallogr. D Biol. Crystallogr.* **2010,** 66, 12-21.

65.   DeLano, W. L. *The PyMol Molecular Visualization System*, Sa Carlos, CA, USA, 2002.

Highlights

- Synthesis of *C*-β-D-glucopyranosyl pyrrole, indole, and imidazole derivatives
- Nanomolar inhibition of human liver glycogen phosphorylase
- X-Ray crystallography of glycogen phosphorylase–*C*-glucosyl imidazole complexes